Effect of the Solvent on Polymer Incompatibility in Solution

L. Zeman and D. Patterson*

Chemistry Department, McGill University, Montreal 110, Quebec, Canada.
Received February 8, 1972

ABSTRACT: It is generally held that the incompatibility of polymers in solution arises from an unfavorable interaction (χ_{23}) between segments of the polymers and is independent of the polymer–solvent interactions (χ_{12} and χ_{13}). This is correct when the polymer–solvent interactions are of equal magnitude, as assumed in Scott's original treatment of such ternary systems. We reexamine the theory, calculating spinodals which show that a small difference in polymer–solvent interactions has a marked effect on polymer incompatibility. This is in agreement with experimental findings of Dondos and others. At high polymer concentration, polymer incompatibility is associated with χ_{23}, but at low concentrations it should be mainly due to the difference between χ_{12} and χ_{13}. Setting $\chi_{23} = 0$ but keeping a sufficient difference between χ_{12} and χ_{13} leads to a closed region of incomplete miscibility within the triangular phase diagram, although the binaries show complete miscibility.

It is a well-known fact that two polymers of different chemical nature are usually incompatible in the absence of solvent. A homogeneous ternary system can be formed by dissolving the polymers (components 2 and 3) in sufficient solvent. However, phase separation occurs when the concentration of total polymer is increased above a critical value. The theoretical work of Scott[1] and Tompa[2] associates these phenomena with an unfavorable interaction ($\chi_{23} > 0$) between the segments of the polymers. Although the critical concentration of total polymer decreases rapidly with increase of the polymer molecular weights, it is apparently independent of the polymer–solvent interactions (χ_{12} and χ_{13}). Thus, the effect of the solvent is merely to dilute the polymers and so diminish the number of unfavorable contacts between polymer segments of different type. This simple and intuitively satisfying result was obtained[1] assuming that the two polymer–solvent interactions were equal, but it was surmised[1,2b] that very similar phase diagrams should be found even when the polymer–solvent interactions are unequal. Some observations of ours on cloud points in very dilute ternary systems under pressure seemed to indicate a strong effect of the solvent. This led us to reexamine the Scott–Tompa theory. We found that phase separation in ternary systems is strongly promoted by any asymmetry in the polymer–solvent interactions ($\chi_{12} \neq \chi_{13}$). Furthermore, this effect seems a more important cause of the polymer "incompatibility" in solution than the interaction between the polymers themselves. Surprisingly, the theory predicts the possibility of polymer incompatibility in solution even when $\chi_{23} = 0$, provided the polymer–solvent interactions are slightly different.

The literature already contains many reports of the effect of solvent on polymer incompatibility. Bank Leffingwell, and Thies[3] observed that polystyrene is visually compatible with poly(vinyl methyl ether) in toluene, benzene, or perchloroethylene, but incompatible in chloroform, methylene chloride, or trichloroethylene. (The differences in compatibility persist even on solvent evaporation, as shown by measured T_g's and dielectric loss factors of the films cast from the different solvents.) Kern[4] measured the critical concentration of a polystyrene–poly(methyl methacrylate) pair in a number of solvents. Values range from 13% (by volume) total polymer in dimethylaniline to only 2.5% in *p*-xylene. This would correspond to a fivefold variation in the value of χ_{23} calculated using the theory. A similar solvent effect has been observed by Paxton[5] for polystyrene–polybutadiene in toluene and carbon tetrachloride, and by Hugelin and Dondos[6] for poly(vinyl-2-pyridine)–poly(methyl methacrylate) in various solvents. The latter authors showed that the critical concentrations of polymer obtained by Kern and by themselves can be correlated with values of $|a_2 - a_3|$, where a is the exponent in the Mark–Houwink intrinsic viscosity–molecular weight relationship. Since the value of a is related to the polymer–solvent interaction paramter, χ_{1i}, Hugelin and Dondos were able to show that an asymmetry of the χ_{1i} parameters increases polymer incompatibility in solution.

Spinodals in the Ternary System

In our investigation of the Scott–Tompa theory, we have avoided the notoriously difficult calculation of the binodals, *i.e.*, phase boundaries separating the stable from metastable and unstable regions. We chose to calculate the spinodals, *i.e.*, boundaries enclosing unstable regions. However, these provide a qualitatively similar phase diagram, and the position of the binodals can be estimated. Others[7] have similarly used spinodals to give an indication of the phase diagram. The critical points, common to binodals and spinodals, may also be obtained, *e.g.*, using eq 7.27 of Tompa. In terms of the Flory–Huggins theory, the equation for the spinodal is[2b]

$$\Sigma m_i\phi_i - 2\Sigma m_i m_j(\chi_i + \chi_j)\phi_i\phi_j + 4m_1m_2m_3(\chi_1\chi_2 + \chi_1\chi_3 + \chi_2\chi_3)\phi_1\phi_2\phi_3 = 0 \quad (1)$$

where

$$2\chi_1 = \chi_{12} + \chi_{13} - \chi_{23} \quad (2)$$

and the other χ_i's are obtained by cyclic interchange of subscripts. The ϕ_i's are the volume fractions, and the m_i's are the numbers of segments in the component molecules. The χ_{ij} interaction parameters correspond to the free energies for the formation of contacts between *segments* of the components, whereas in Flory's nomenclature the contact involves the whole of the molecule of the first component, *i.e.*, χ_{ij}(Flory) = $m_i\chi_{ij}$(Scott–Tompa).

Figure 1 shows the spinodals[8] with $m_1 = 1$, for two polymers

(1) R. L. Scott, *J. Chem. Phys.*, **17**, 279 (1949).
(2) (a) H. Tompa, *Trans. Faraday Soc.*, **45**, 1142 (1949); (b) "Polymer Solutions," Butterworths, London, 1956, p 185; (c) ref 2b, p 195.
(3) M. Bank, J. Leffingwell, and C. Thies, *Macromolecules*, **4**, 43, (1971).
(4) R. J. Kern, *J. Polym. Sci.*, **21**, 19 (1956).
(5) T. R. Paxton, *J. Appl. Polym. Sci.*, **7**, 1499 (1963).
(6) C. Hugelin and A. Dondos, *Makromol. Chem.*, **126**, 206 (1969).
(7) (a) H. A. G. Chermin, Ph.D. Thesis, University of Essex, Colchester, England, 1971; (b) R. Koningsveld, H. A. G. Chermin, and M. Gordon, *Proc. Roy. Soc., Ser. A*, **319**, 331 (1970).
(8) Details of the calculations and computer programs may be obtained from the authors.

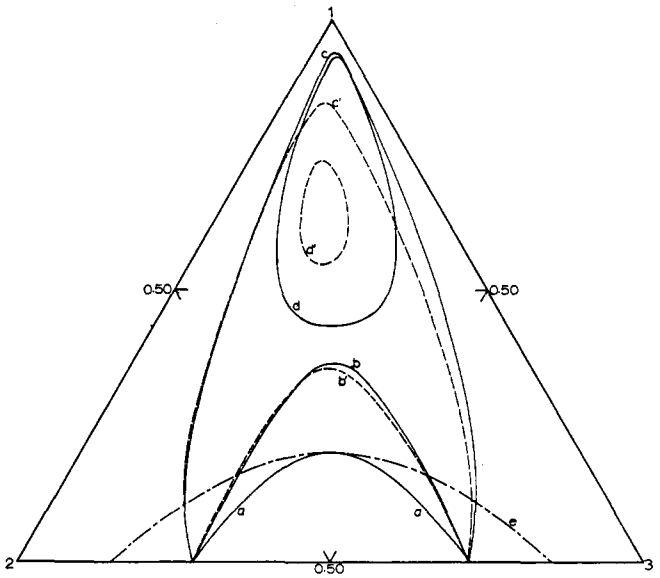

Figure 1. Calculated spinodals for a ternary system: solvent (1), polymer (2), and polymer (3). Values of $m_1 = 1$ and $m_2 = m_3 = 1000$ are taken for all curves. For spinodals a, b, and c, $\chi_{23} = 0.0025$, and the pairs of interaction parameters χ_{12}, χ_{13} are as follows: (a) 0.40, 0.40; (b) 0.40, 0.45; (b′) 0.40, 0.35; (c) 0.40, 0.50; (c′) 0.40, 0.30. For spinodals d and d′, $\chi_{23} = 0.0$ and χ_{12}, χ_{13} are the same as for (c) and (c′). Curve e is a binodal calculated with the same choice of parameters as for spinodal a. Solution compositions are in volume fractions.

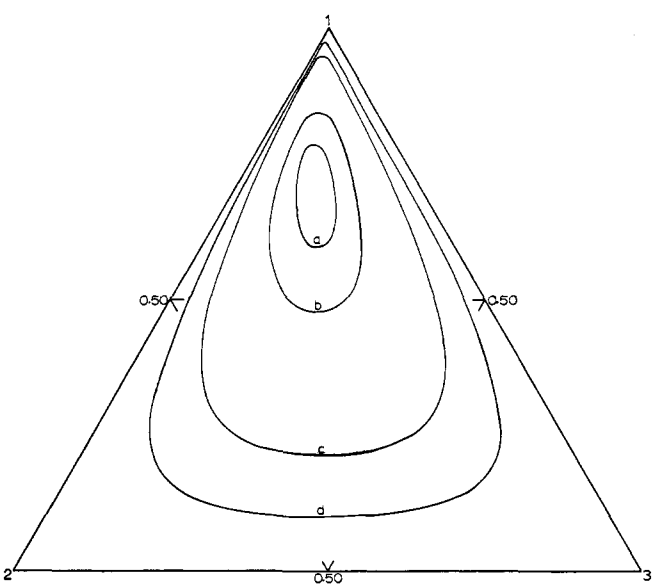

Figure 2. Calculated spinodals for a ternary system: solvent (1), polymer (2), and polymer (3), with $\chi_{23} = 0.0$ and χ_{12}, χ_{13} equal to 0.50, 0.30; $m_1 = 1$ and the values of $m_2 = m_3$ are as follows: (a) 220; (b) 250; (c) 500; (d) 1000. At $m = 200$ complete miscibility is observed. Solution compositions are in volume fractions.

characterized by $m_2 = m_3 = 10^3$, corresponding to equal molecular weights of $\sim 10^5$. The interaction parameter between polymer segments $\chi_{23} = 0.0025$. Curve a shows the spinodal calculated under the symmetrical conditions assumed in the original Scott treatment, $\chi_{12} = \chi_{13}$. As found there, the spinodal is independent of the χ_{1i}'s, provided they are equal. A typical value of the χ_{1i} for a good solvent would be 0.40. The almost identical spinodals b and b′ show that even a small disparity, *i.e.*, $\chi_{12} = 0.40$, $\chi_{13} = 0.40 \pm 0.05$,

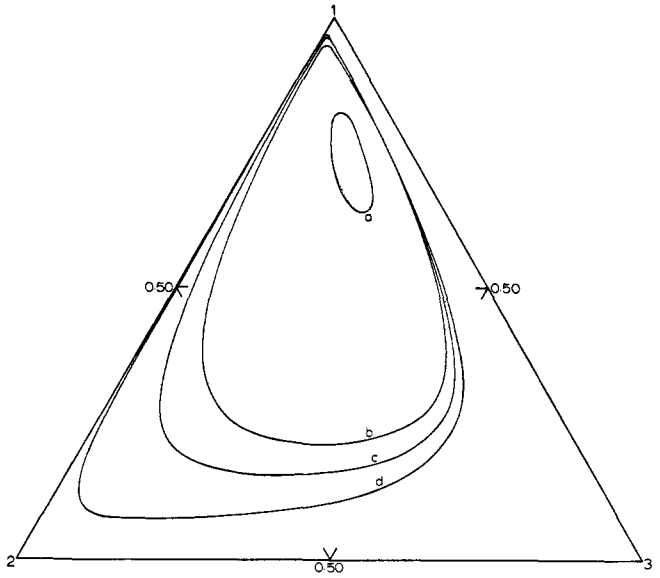

Figure 3. The values of χ_{23} and χ_{12}, χ_{13} are as in Figure 2; $m_1 = 1$, and the values of m_2, m_3 are as follows: (a) 500, 100; (b) 500, 500; (c) 500, 1000; (d) 500, 10,000. Solution compositions are in volume fractions.

greatly enlarges the region of incomplete miscibility. It is of interest that increasing the quality of the solvent for polymer 3 produces almost the same effect as decreasing it. Spinodals c and c′ introduce a larger difference in χ_{1i}, but one which is still comparable with the variations of the χ values encountered in actual systems: $\chi_{12} = 0.40$, $\chi_{13} = 0.40 \pm 0.10$. It is clear that the magnitude of the average polymer–solvent interaction has a considerably smaller effect on the spinodal than the difference in the interactions.

We now calculate the spinodals under the same conditions except that $\chi_{23} = 0$. There is now no polymer incompatibility in the absence of the solvent, nor in the solution when the χ_{1i}'s are equal, *i.e.*, spinodal a disappears. The same is true of spinodals b and b′, where the polymer incompatibility is confined to the region of high polymer concentration. However, if the difference in polymer–solvent interactions is larger, extending polymer incompatibility to low polymer concentration, a region of incompatibility remains when $\chi_{23} = 0$, and in fact when $\chi_{23} < 0$. Spinodals d and d′ correspond to c and c′, except that $\chi_{23} = 0$. Eliminating χ_{23} has caused the region of incompatibility to disappear at high concentration but not at low. The spinodals are closed loops which do not touch the edges of the triangular phase diagram, *i.e.*, the binaries are complete miscible.[9] In these model systems, but probably also in real systems, limited miscibility at low concentration is an effect of unequal polymer–solvent interactions, while at high concentration it reflects the unfavorable polymer–polymer interaction.

(9) There may be other reasons for the instability of a ternary system while the binaries remain stable, *i.e.*, the occurrence of a closed loop. J. L. Meijering, *Philips Res. Rep.*, **5**, 333 (1950); **6**, 183 (1951), has given a general treatment of the phenomenon in regular solutions of small molecules. It can also occur in a system containing one polymer and two solvents. If the solvents interact strongly between themselves ($\chi < 0$), they will not easily tend to form contacts with the polymer. It is thus possible for the two polymer–solvent binaries to be stable but not the ternary mixture. Such systems have been studied by G. Gee, *Trans. Faraday Soc.*, **40**, 468 (1944), and by A. Dondos, *C. R. Acad. Sci.*, **267**, 370 (1968). Tompa[26] mentions a case of a closed loop in a polymer-solvent-poor solvent system. If the two solvents are almost at the point of phase separation ($\chi \sim 2$), the introduction of the third component can cause instability. A disparity in the polymer–solvent interactions apparently enhances the effect, and the behavior may be similar to that discussed in this article.

Dependence on Polymer Molecular Weight

The effect of unequal polymer–solvent interactions, like that of an unfavorable polymer–polymer interaction, manifests itself for high polymer molecular weight. The effects shown in Figure 1 become more striking on raising the value of m for the polymers from 10^3 to 10^4, corresponding to a molecular weight of about 10^6. Incompatibility of the polymers in solution remains when $\chi_{23} = 0$ if the disparity in polymer–solvent interaction parameters is as little as 0.03. On the other hand, Figure 2 shows that, even when $|\chi_{12} - \chi_{13}|$ is fairly large, *i.e.*, 0.2, the closed immiscibility loop rapidly disappears when the polymer molecular weight becomes small. Figure 3 demonstrates the effect of unequal molecular weights of the two polymers. Increasing the molecular weight of one of the polymers enlarges the region of polymer incompatibility, but does so mainly in the region of high concentration of the polymer of lower molecular weight. A similar effect is found in the case treated by Scott, where the χ_{1i}'s are equal, and polymer incompatibility is due to χ_{23}. There also, the higher molecular weight polymer expels the lower from the solution.

Critical Points and the Binodals

The evolution of critical points in Figure 1 is of interest. Each of the spinodals a, b, and c shows only one critical point, approximately at the point on the spinodal corresponding to lowest total polymer concentration, the critical concentration usually measured. The closed loops in Figure 1 (and 2) each have two critical points. One is at low polymer concentration and corresponds to those on spinodals a, b, and c. The other is at high polymer concentration and may be thought of as having arisen from a critical point in the pure 2–3 binary. Starting with spinodals a, b, and c in Figure 1, and decreasing the value of χ_{23}, the points of intersection of the spinodals with the base of the triangular phase diagram come together to give the critical point of the pure 2–3 binary. The spinodals b and c have now changed into loops touching the base of the phase diagram at this critical point. With further decrease of χ_{23}, the loops detach themselves from the base of the phase diagram, but retain the critical point at the high polymer concentration extremity of the loop. The spinodal b becomes smaller and finally disappears, its two critical points coalescing, before χ_{23} reaches zero. The above discussion indicates that a closed loop cannot be accompanied by phase separation in the 2–3 binary.

Figure 1 shows the binodal in the case of equal χ_{1i}. The corresponding binodals in the case of the unequal χ_{1i} must be similar smooth curves starting from the critical points at the low polymer concentration tops of the spinodals. They must pass outside of the spinodals to cut the base of the triangular phase diagram at the same points as the binodal in the case of equal χ_{1i}. In the case of the closed solubility loops of Figures 1, 2, and 3, the positions of the binodals may be estimated, since they pass outside of the loops, do not touch the edges of the phase diagram, and are tangential to the loops at the two critical points.

Case of Incomplete Miscibility in the Polymer–Solvent Binaries

Figure 4 illustrates the effect of asymmetry of the polymer–solvent interaction in cases where the χ_{1i}'s are sufficiently large to cause phase separation in the polymer–solvent binaries, associated with an upper or a lower critical solution temperature. We have retained the same difference of $|\chi_{12} - \chi_{13}|$ as in Figure 1, spinodal d′, *i.e.*, $\chi_{12} = 0.40$, $\chi_{13} = 0.30$. Spinodal a of Figure 4 is identical with d′ in Figure 1. Then χ_{12} and χ_{13}

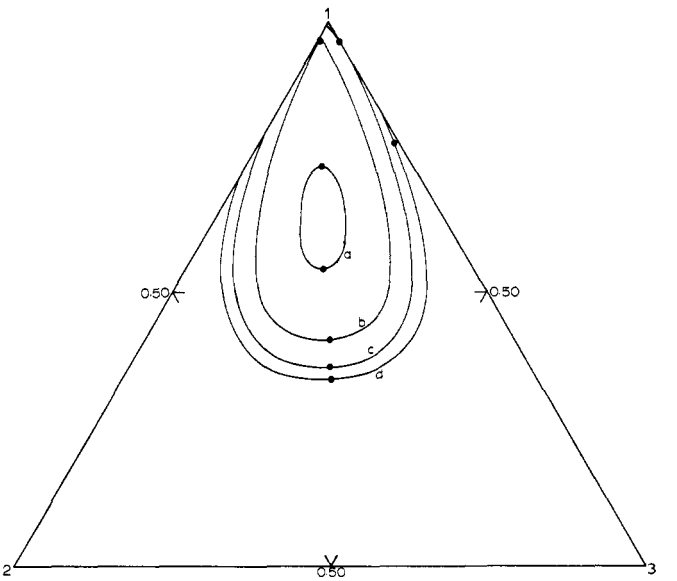

Figure 4. Calculated spinodals and the critical points for the ternary system: solvent (1), polymer (2), and polymer (3), with $\chi_{23} = 0.0$, and the following pairs of interaction parameters χ_{12}, χ_{13}: (a) 0.40, 0.30; (b) 0.532, 0.432; (c) 0.632, 0.532; (d) 0.70, 0.60; $m_1 = 1$ and $m_2 = m_3 = 1000$ for all curves. The critical points which lie within the phase diagram are shown as dots. Solution compositions are in volume fractions.

are increased by successive increments so that phase separation occurs first in the 1–2 binary and then in both the 1–2 and 1–3 binaries. This process corresponds to changing the temperature to approach a critical solution temperature in a binary. (If the interaction parameters are decreased, the loop disappears at $\chi_{12} = 0.38$, $\chi_{13} = 0.28$).

The spinodals show nothing remarkable, but the evolution of the positions of the critical points is of interest. The critical point at high polymer concentration remains at the bottom of the successive spinodals. The critical point at low polymer concentration reaches the 1–2 binary (edge of the phase diagram) in spinodal b, where it is the well-known critical point given by the Flory–Huggins critical conditions: $\chi_{1i} = (1/2)\{1 + (m_1/m_i)^{1/2}\}^2$; $\phi_i = \{1 + (m_i/m_1)^{1/2}\}^{-1}$. These yield $\chi_{1i} = 0.532$ in the present case. When $\chi_{12} > 0.532$, this critical point lies outside of the phase diagram. Until $\chi_{12} = 0.632$, $\chi_{13} = 0.532$, therefore, the spinodals have only one critical point inside the phase diagram. With this pair of χ_{1i} a new critical point appears on the 1–3 binary. Increasing the χ_{1i} splits this point into two, one just inside the diagram, but the other outside. Thus, spinodal d shows only two critical points in Figure 3.

Discussion

We have attempted unsuccessfully to find experimental examples of the closed-loop spinodals. Our attempt was rather cursory, but at least it seems that the loops must be, in practice, a rare phenomenon. It is probable that the difference in nature between the polymers, required to furnish the difference in χ_{1i}, also suffices to give an important χ_{23}. Hence, the loops would be extended into the region of high polymer concentration, to produce spinodals of the type shown in Figure 1, curves b and c. This view is supported by an argument based on the solubility parameter theory. For the polymer–solvent interactions, we have

$$\chi_{1i}(\text{Flory}) = m_1\chi_{1i}(\text{Scott–Tompa}) = \frac{V_1}{RT}(\delta_1 - \delta_i)^2 + \beta \quad (3)$$

For the interaction of the two polymers

$$\chi_{23}(\text{Flory}) = m_2\chi_{23}(\text{Scott–Tompa}) = \frac{V_2}{RT}(\delta_2 - \delta_3)^2 \quad (4)$$

Then, one finds

$$\chi_{23} = \frac{(\chi_{12} - \chi_{13})^2}{(\delta_2 + \delta_3 - 2\delta_1)^2}\frac{RT}{v} \quad (5)$$

where v is the molar volume of the segments in the solvent molecules. In the present work, $m_1 = 1$, so that $v \sim 100$ cm^3/mol. We then have

$$\chi_{23} \sim (\chi_{12} - \chi_{13})^2 \quad (6)$$

An inspection of the χ values in Figure 1, curves b and c, and for other spinodals not reported here, indicates that if eq 6 is correct, closed immiscibility loops should not be generally found, but rather spinodals like curves b and c in Figure 1. Possibly the loops could occur in a special case with two polymers of very similar chemical nature, which would minimize χ_{23}, but of different flexibilities, which would produce different free volume or equation of state contributions in χ_{12} and χ_{13}.

Koningsveld and collaborators[7] have studied a system which shows a closed immiscibility loop: linear polyethylene–crystallizable polypropylene–diphenyl ether. They indicate that other such systems have been found, and point out that polymer incompatbility in solution does not necessarily imply incompatibility in the absence of solvent. Since, however, the two polymer–solvent binaries phase separate at about the same temperature, one would expect the χ_{1i}'s to be almost identical. It is possible, therefore, that this closed loop may have a different origin than that described in the present paper.

We feel then that our main result is a theoretical support for the experimental finding of Dondos and others that polymer incompatibility in solution is increased when the polymer–solvent interactions are different. Another area where the solvent effect could be important is in the "segregation" of the blocks within isolated block copolymer macromolecules, and recent work by Dondos[10] may indeed show such an effect.

Acknowledgment. We are grateful to the Petroleum Research Fund, administered by the American Chemical Society, for support of our research and to the National Research Council of Canada for a scholarship to L. Z. We thank Dr. W. Brostow of the Université de Montréal for stimulating discussion and preliminary work on this problem.

(10) A. Dondos, *Makromol. Chem.*, **147**, 123 (1971).

Efficient Computer Simulation of Polymer Conformation. I. Geometric Properties of the Hard-Sphere Model

Steven D. Stellman* and Paul J. Gans

Department of Chemistry, New York University, New York, New York 10003.
Received November 19, 1971

ABSTRACT: A system of efficient computer programs has been developed for simulating the conformations of macromolecules. The conformation of an individual polymer is defined as a point in conformation space, whose mutually orthogonal axes represent the successive dihedral angles of the backbone chain. The statistical-mechanical average of any property is obtained as the usual configuration integral over this space. A Monte Carlo method for estimating averages is used because of the impossibility of direct numerical integration. Monte Carlo corresponds to the execution of a Markoffian random walk of a representative point through the conformation space. Unlike many previous Monte Carlo studies of polymers, which sample conformation space indiscriminately, importance sampling increases efficiency because selection of new polymers is biased to reflect their Boltzmann probabilities in the canonical ensemble, leading to reduction of sampling variance and hence to greater accuracy in given computing time. The simulation is illustrated in detail. Overall running time is proportional to $n^{5/4}$, where n is the chain length. Results are presented for a hard-sphere linear polymer of n atoms, with free dihedral rotation, with n = 20–298. The fraction of polymers accepted in the importance sampling scheme, f_A, is fit to a Fisher–Sykes attrition relation, giving an effective attrition constant of zero. f_A is itself an upper bound to the partition function, Q, relative to the unrestricted walk. The mean-squared end-to-end distance and radius of gyration exhibit the expected exponential dependence, but with exponent for the radius of gyration significantly greater than that of the end-to-end distance. The 90% confidence limits calculated for both exponents did not include either $^6/_5$ or $^4/_3$, the lattice and zero-order perturbation values, respectively. A self-correcting scheme for generating coordinates free of roundoff error is given in an Appendix.

The Monte Carlo method[1] was firmly established by Wall and his successors[2–10] as a valuable tool for investigating the geometric and thermodynamic properties of polymers. The majority of previous Monte Carlo studies have been confined to the exploration of extremely simple models, such as random walks on lattices. In this paper we offer a more complete model of polymeric systems which includes lattice as well as off-lattice polymers on special cases, an ideal frame-

* Address correspondence to this author at the Department of Biochemical Sciences, Frick Chemical Laboratory, Princeton University, Princeton, N. J. 08540.

(1) J. M. Hammersley and D. C. Handscomb, "Monte Carlo Methods," Wiley, New York, N. Y., 1964.

(2) (a) F. T. Wall, L. A. Hiller, Jr., and D. J. Wheeler, *J. Chem. Phys.*, **22**, 1036 (1954); (b) F. T. Wall, L. A. Hiller, Jr., and W. F. Atchison, *ibid.*, **23**, 913, 2314 (1955); **26**, 1742 (1957).

(3) F. T. Wall and J. Mazur, *Ann. N. Y. Acad. Sci.*, **89**, 608 (1961).

(4) (a) F. T. Wall, S. Windwer, and P. J. Gans, *J. Chem. Phys.*, **38**, 2220 (1963); (b) *ibid.*, **38**, 2228 (1963).

(5) J. Mazur and F. L. McCrackin, *ibid.*, **49**, 648 (1968).

(6) E. Loftus and P. J. Gans, *ibid.*, **49**, 3828 (1968).

(7) P. J. Gans, *ibid.*, **42**, 4159 (1965), and references cited therein.

(8) C. Domb, *Advan. Chem. Phys.*, **15**, 229 (1969).

(9) J. Mazur, *ibid.*, **15**, 261 (1969).

(10) K. K. Knaell and R. A. Scott, *J. Chem. Phys.*, **54**, 566 (1971).